UCRL-17105

University of California

Ernest O. Lawrence Radiation Laboratory

THE EFFECT OF PLASTIC INSTABILITY ON CREEP OF MgO SINGLE CRYSTALS IN COMPRESSION

TWO-WEEK LOAN COPY

This is a Library Circulating Copy which may be borrowed for two weeks. For a personal retention copy, call Tech. Info. Division, Ext. 5545

Berkeley, California

DISCLAIMER

This document was prepared as an account of work sponsored by the United States Government. While this document is believed to contain correct information, neither the United States Government nor any agency thereof, nor the Regents of the University of California, nor any of their employees, makes any warranty, express or implied, or assumes any legal responsibility for the accuracy, completeness, or usefulness of any information, apparatus, product, or process disclosed, or represents that its use would not infringe privately owned rights. Reference herein to any specific commercial product, process, or service by its trade name, trademark, manufacturer, or otherwise, does not necessarily constitute or imply its endorsement, recommendation, or favoring by the United States Government or any agency thereof, or the Regents of the University of California. The views and opinions of authors expressed herein do not necessarily state or reflect those of the United States Government or any agency thereof or the Regents of the University of California.

UCRL-17105

Research and Development

UNIVERSITY OF CALIFORNIA

Lawrence Radiation Laboratory
Berkeley, California

AEC Contract No. W-7405-eng-48

THE EFFECT OF PLASTIC INSTABILITY ON CREEP OF MgO SINGLE CRYSTALS IN COMPRESSION

Donald Riddick Cropper
(M. S. Thesis)

September 2, 1966

THE EFFECT OF PLASTIC INSTABILITY ON CREEP OF MgO SINGLE CRYSTALS IN COMPRESSION

Contents

Abstract v

I. Introduction 1

A. Literature Survey 1

B. Plastic Buckling of Columns 2

II. Experimental Procedure 9

A. Materials 9

B. Apparatus 10

C. Test Procedure 11

III. Results and Discussion 13

A. Effect of Buckling on Strain Rate 13

B. Observations of Microstructure 22

C. Effect of End Constraints 25

D. Stress Distribution in a Buckled Column 27

E. Surface Condition 30

F. Mechanisms 32

1. Stress Exponent 32

2. Activation Energy 33

IV. Conclusions 36

Acknowledgments 38

References 39

THE EFFECT OF PLASTIC INSTABILITY ON CREEP OF MgO SINGLE CRYSTALS IN COMPRESSION

Donald Riddick Cropper

Inorganic Materials Research Division, Lawrence Radiation Laboratory, and Department of Mineral Technology, College of Engineering, University of California, Berkeley, California

September 2, 1966

ABSTRACT

The creep of MgO single crystals loaded in compression was studied under conditions where plastic buckling was likely to occur. The degree of end constraint characteristic of these tests strongly affects the possibility of buckling. Experiments suggest that buckled columns creep at a lower rate than do columns that remain straight. At temperatures around 1300°C and above, the creep rate appears to be particularly sensitive to the nature of the crystal surface prior to deformation. At 1200°C the stress dependence of the creep strain rate can be represented as a power law with a stress exponent of 4.7. This is in reasonable agreement with Chang's theory of creep by diffusion controlled dissolution of dislocation dipoles and loops.

I. INTRODUCTION

A. Literature Survey

During the decade since the work of Parker et al.[1,2] the plastic deformation of magnesium oxide single crystals has been subjected to intensive study. The early interest was in the room temperature ductility of MgO but since that time studies have extended knowledge to temperatures above 2000°C. Significant contributions to the understanding of deformation phenomena in MgO have been made by Stokes and co-workers at the Honeywell Research Center.[3,4,5,6] Extensive work in this laboratory by Pask and others led directly to the study described herein.[7,8,9,10]

Despite the efforts directed toward understanding the mechanical behavior of MgO, literature concerning the high temperature creep behavior is meager. Hulse and Pask[8] reported preliminary creep studies of <001> oriented single crystals in compression at temperatures between 800° and 1000°C. They found large instantaneous plastic deformation followed by slow constant-rate creep. Cummerow[11] studied creep of MgO single crystals subjected to three point bending between 1450° and 1700°C. He concluded that creep in MgO is a thermally activated process with an activation energy ranging from 3.5 to 7 eV (81 - 162 kcal/mole). Cummerow also described the variation of strain rate with applied stress by a power law with an exponent varying from 4 to 7 thus lending support to the Weertman theory of steady state creep by edge dislocation climb. Neiman and Rothwell[13,14] studied creep of MgO single crystals in three point bending below 1100°C and above 1300°C, including extensive observations on modifications of creep behavior by a d.c. electric field. They report that creep at 1000°C is cross slip controlled while creep between

1300° and 1630°C is best described by diffusion controlled climb of edge dislocations over obstacles. More recently Rothwell[15] analyzed the low temperature results, deriving analytical expressions for the creep strain-rate-time dependence in agreement with experiments at 1000°C.

The principal goal in this work was to provide a detailed study of the creep in compression of <001> oriented MgO single crystals between 1000° and 1300°C. Compression loading has been used in this laboratory for a number of years in mechanical behavior studies, primarily in constant stress rate tests. Provided no buckling of the specimen occurs, the stress distribution in a compressed rectangular parallelepiped is both uniaxial and uniform. In addition, no special grips or specimen geometry are required; for a <001> stress axis the specimen can be prepared for testing simply by cleaving. Difficulties in constraining the ends of the crystals have been noted by Hulse and Pask[8] and by Copley and Pask.[10] Translation of the specimen ends across the faces of the loading rams was observed and attributed to lateral forces developed by resistance to slip intersections on {110} planes at 90°. This investigator also encountered similar problems but attributes them primarily to the additional complications arising from the plastic instability or buckling of the slender columns typically used in these tests. A digression on the subject of plastic buckling of columns loaded in compression thus would be in order at this point.

B. Plastic Buckling of Columns

Let us consider first the classical example of a two hinged bar of constant cross-section, initially ideally straight and homogeneous, subjected to an exactly axial load as shown in Figure 1. The smallest value

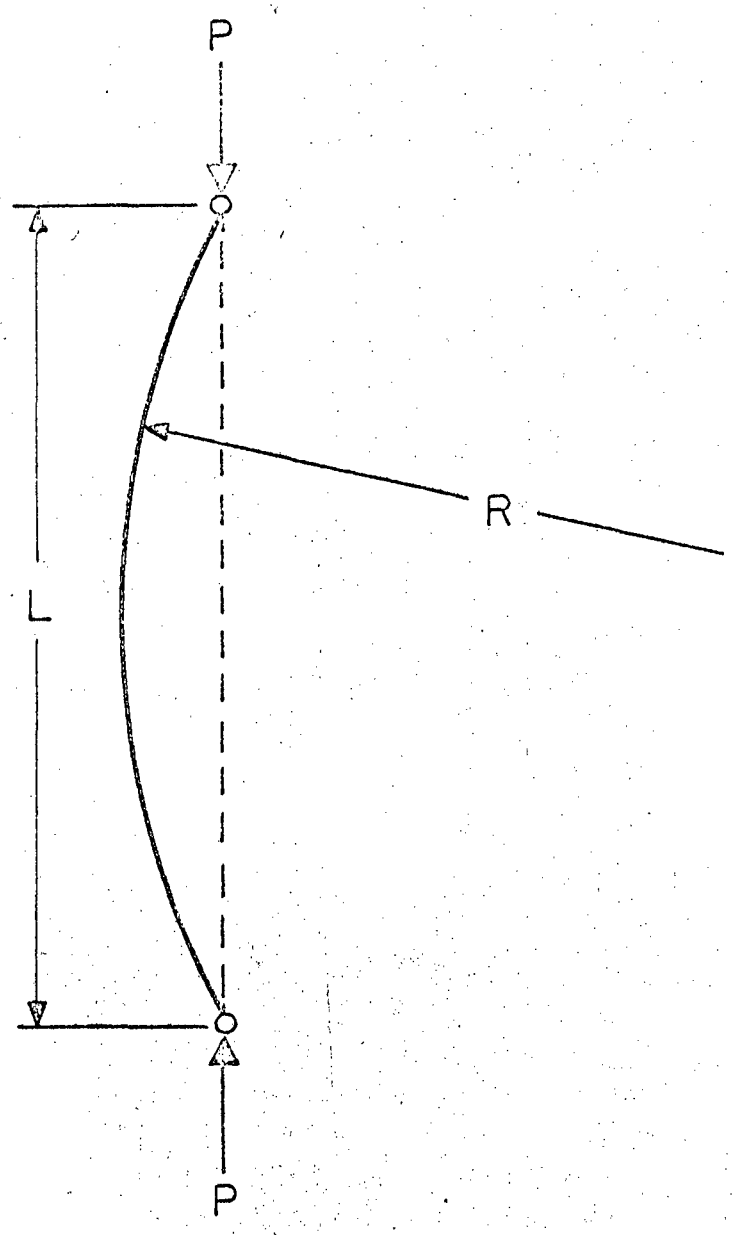

Fig. 1. Deflection of a buckled bar pinned at both ends.

of P, the applied load, for which a buckled configuration is possible is given by the well known Euler value

$$P = \frac{\pi^2 EI}{L^2} \tag{1}$$

where E is the elastic modulus and I is the moment of inertia of the cross-section with respect to its centroidal axis about which rotation occurs.

Now, if a material behaves plastically, i.e., if the stress in the compressed bar increases beyond the yield point before the Euler load is reached, two situations may be obtained. In the first case small initial perturbations in alignment of the stress axis cause the axial load and the resulting bending moment to undergo simultaneous increases. In the second case the axial load increases to the Euler value, at which time the bending moment appears. During the latter part of loading a strain reversal occurs over part of the cross-section. If, for simplicity, we assume we are loading a column of a material with a compressive stress-strain curve approximated by two straight lines as shown in Fig. 2, then the critical loads for buckling will be given by

$$P_t = \frac{\pi^2 BI}{L^2} \quad \text{(Engesser load)} \tag{2}$$

$$P_r = \frac{\pi^2 E_r I}{L^2} \quad \text{(Reduced modulus load)} \tag{3}$$

for the two cases above, respectively. The quantity B in Eq. (2) is simply the slope of the second straight-line branch of the diagram which represents, in an idealized fashion, the strain hardening region. The modulus E_r in Eq. (3) is known as the reduced modulus; for a rectangular

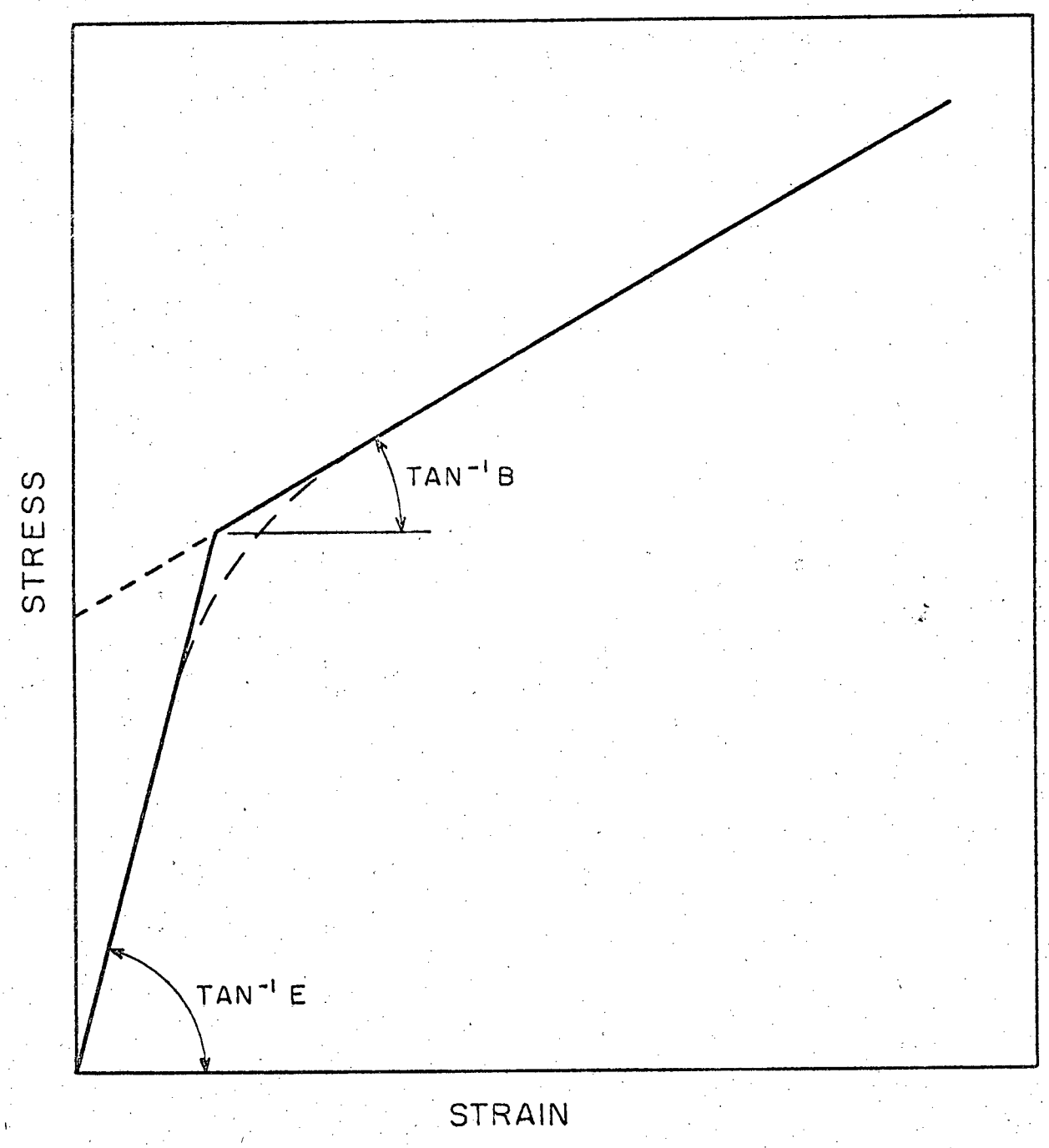

Fig. 2. Stress-strain curve approximated by two straight lines.

cross section its value is given by

$$E_r = \frac{4EB}{(\sqrt{E} + \sqrt{B})^2} \tag{4}$$

A modification of the Engesser load that is frequently made for a real material that strain-hardens nonlinearly is to replace B in Eq. (2) with E_t, the tangent modulus or slope of the stress-strain curve at the stress involved. Equation (2) can then be written

$$P_t = \frac{\pi^2 E_t I}{L^2} \tag{5}$$

The significance of this formula was stated by Shanley.[17] Any <u>real</u> column having some initial perturbance, will follow the first equilibrium path and will buckle when the load reaches P_t, Eq. (5), because E_t is less than E_r. A significant amount of test data confirms this conclusion.

The buckling formulae presented above in Eqs. (1), (2), (3), and (5) were all derived for columns pinned at the ends. A word as to the effect of other end conditions is thus in order. Three cases which are commonly observed in practice are shown in Fig. 3. For a column built in at one end and free at the other, Fig. 3(a), the critical load is

$$P_t = \frac{\pi^2 E_t I}{4L^2} \tag{6a}$$

For a column fixed at one end and pinned at the other, Fig. 3(b), the critical load is

$$P_t = \frac{2.05\ \pi^2 E_t I}{L^2} \tag{6b}$$

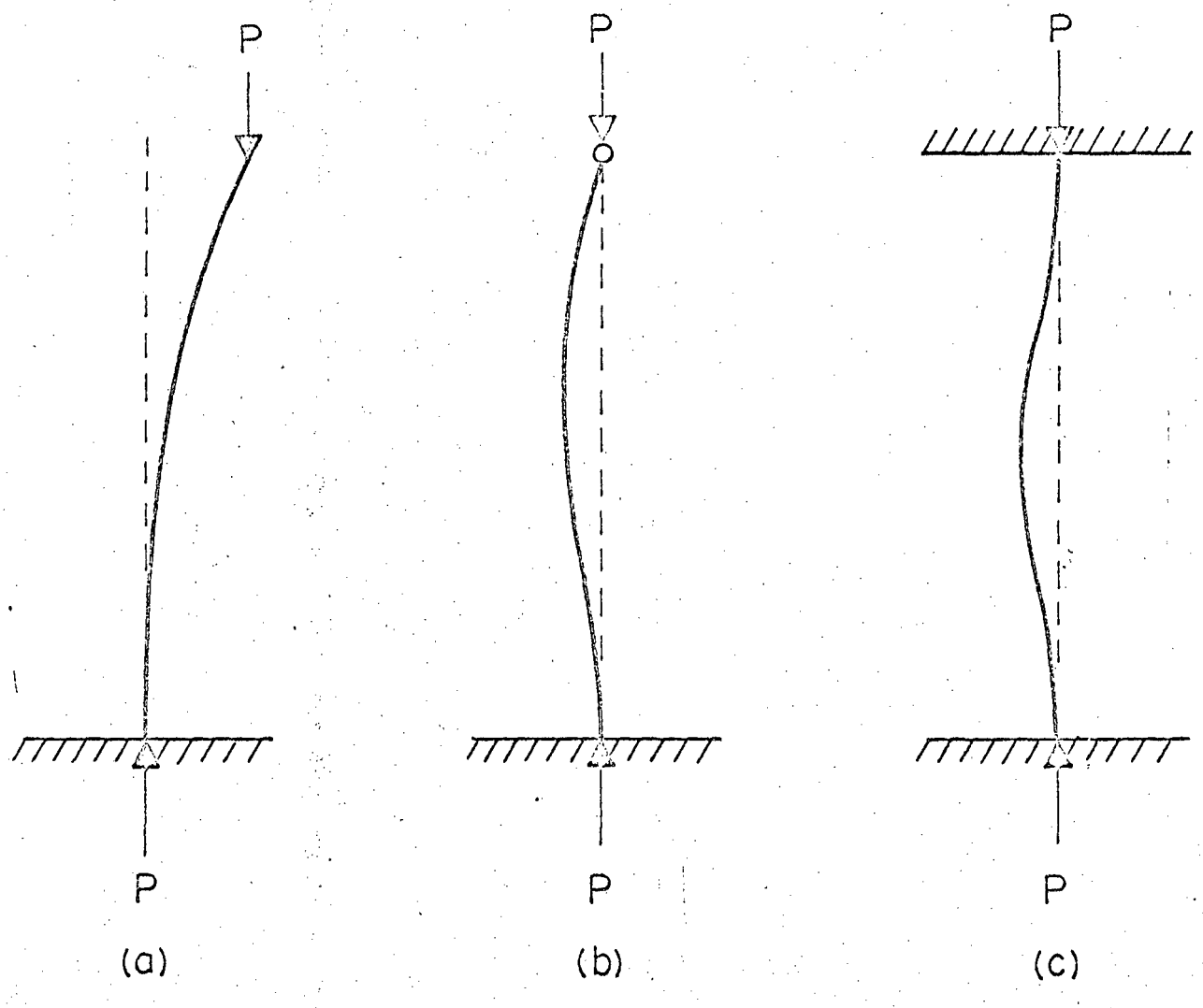

Fig. 3. Deflection of buckled bars with various end constraints.

And a column fixed at both ends, Fig. 3(c), has a critical load of

$$P_t = \frac{4\pi^2 E_t I}{L^2} \tag{6c}$$

According to Popov,[18] when there is uncertainty regarding the end conditions of real columns, the ends are most often assumed to be pinned, in which case Eq. (5) applies. Additional comments with particular regard to the experimental conditions in this study will be made later.

The next section of this thesis concerns itself primarily with experimental procedure, i.e. materials, apparatus and testing details. This section will be followed by one on the experimental results and a discussion of the results in the light of the comments on buckling presented above. Finally, the conclusions that can be drawn from this work will be stated.

II. EXPERIMENTAL PROCEDURE

A. Materials

Large grained polycrystalline aggregates of MgO formed by slow cooling in a carbon arc furnace were purchased from Muscle Shoals Electrochemical Corp., Tuscumbia, Alabama. Semi-quantitative spectrographic analysis by American Spectrographic Laboratories, San Francisco, California, determined the crystals to be 99.94% MgO. Typical values for impurities detected, reported as oxides of the elements indicated, were Ca (0.04%), Fe (0.008%), Cr (0.002%), Mn (0.001%), Al (0.007%), Cu (<0.001%) and Ni (<0.002%).

Single crystal specimens in the form of rectangular parallelepipeds typically 1.0 x 0.225 x 0.225 inches were cleaved along {100} faces. The loading ends were then ground flat, parallel to each other and perpendicular to the load axis, <001>, by mounting in a specially prepared steel yoke and polishing on Type 1 Emery Polishing Paper. The specimen dimensions were then accurately determined and two small divots, nominally one half inch apart, were made on the center of one face with a No. 80 steel twist drill to serve as a gauge length. Varying degrees of surface damage were obtained by one of the following procedures. Most tests were performed on crystals in the "as cleaved" condition. Etching with a two part H_3PO_4:1 part H_2SO_4 solution at room temperature revealed etch pits indicative of a moderate degree of surface damage realized through normal handling. Some crystals were polished as long as five minutes in H_3PO_4 at 155°C in order to remove most of the surface damage. Other crystals were subjected to this polishing procedure and subsequently heavily damaged by dropping No. 120 SiC grit

repeatedly on the side faces. Such treatment was observed to introduce a large number of rosette-like arrays of dislocations to the surface.

B. Apparatus

The creep apparatus employed in this study was essentially the same machine described as Apparatus II by Hulse and Copley.[19] Some modifications were made in that the loading rams were high density Al_2O_3 rather than SiC, and an improved automatic controller was employed to control the furnace temperature. The MgO crystals were compressed by the alumina rams which were constrained so that their axes remained aligned during motion. Tests were performed at constant load, the load being applied through a lever system. Constant loading rates were obtained by regulating the flow of water into a large tank suspended from the end of the lever system. The final value of load was attained in from three to ten minutes.

One feature of this apparatus which affects the buckling behavior of the specimens is an inherent instability in the loading rams. The bottom Al_2O_3 cylinder is fixed quite securely to the base of the apparatus and does not move. The upper ram is fixed to the lever system and moves vertically as the load is applied. Linear ball bearing bushings are employed to position the ram and insure that its motion is restricted to only the axial direction. However, the bushing nearest the loading surface is thirteen inches away. Thus the loading system itself, behaving as a slender column loaded elastically in compression, can bend a small amount during the application of the load. The situation described is far enough removed from "ideality" that the first case of plastic buckling described in the introduction would be expected to

occur with a simultaneous application of axial load and bending moment.

C. Test Procedure

After the crystals were prepared for testing as described above, they were placed between two dense alumina buttons, nominally 3/8 inch thick and 3/4 inch in diameter. Small squares of 0.001 inch thick platinum sheet were placed between the specimen ends and the alumina buttons to act as reaction barriers. The buttons and crystal were then positioned between the rams and a small pre-load, usually about 15 pounds, was applied to hold the test assembly in position. Spring-loaded sapphire rods were then positioned in the divot holes so that the change in distance between the holes could be transmitted via a double lever system to a Shaevitz Linear Variable Differential Transformer. The differential voltage from the transformer was amplified by a Daytronic Model 300C amplifier. The amplified signal was then received and plotted by a Brown Electronik recording potentiometer as deflection versus time.

The applied stresses were calculated from the applied load on the basis of the cross-sectional area of the specimen before deformation. Values of strain were reported as engineering strain, e, where

$$e = \frac{\Delta \ell}{\ell_o} \tag{7}$$

Here ℓ_o is the original room temperature gauge length and $\Delta \ell$ is the observed change in spacing of the divots. This procedure is in contrast to reporting the true strain, ε, given by

$$\varepsilon = \int_{\ell_o}^{\ell} \frac{d\ell}{\ell} = \ln (1 + e) \tag{8}$$

In this expression e and ℓ_o are defined as for Eq. (7) and ℓ is the instantaneous gauge length. A significant difference between e and ε occurs only at high strains. For example, if e is 0.10, the value of ε calculated from Eq. (8) is 0.0953, a difference of only 4.7%.

III. RESULTS AND DISCUSSION

A. Effect of Buckling on Strain Rate

Compression stress-strain curves obtained previously by Copley[10] were used to calculate the critical loads for buckling in the temperature range studied here. Values of the tangent modulus, E_t, were obtained directly from the curves shown in Fig. 4 at each temperature and stress level desired. Using these values and a normal specimen geometry, i.e., 1.0 x 0.225 x 0.225 inches, the critical buckling loads as calculated from Eq. (5) are shown in Table 1.

Table I. Critical buckling loads for crystals deformed between 1000° and 1300°C

Temperature	Stress (psi)	Equivalent load (lb)	P_t, buckling load (lb)
1000°C	6000	304	221
	8000	406	
1100°C	6000	304	210
	8000	406	
1200°C	6000	304	156
	8000	406	
1300°C	6000	304	311
	8000	406	183

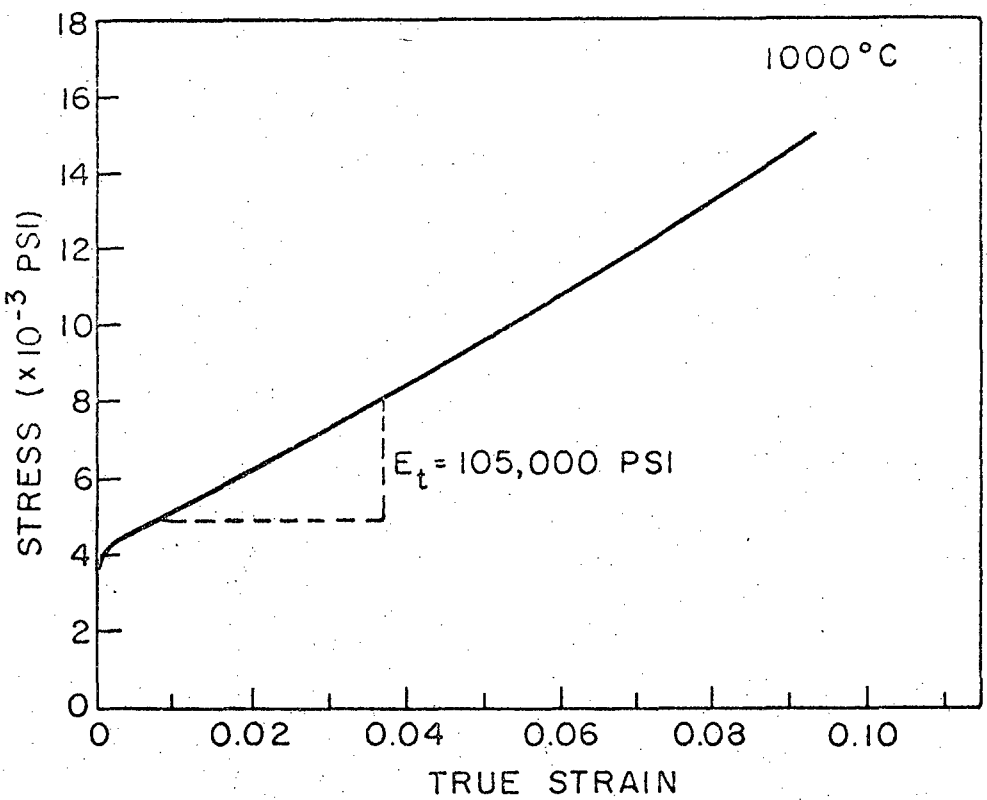

(a)

Fig. 4. Stress-strain curves at 1000°, 1100°, 1200° and 1300°C for single crystals compressed in an <001> direction. Values of the tangent modulus, E_t, are shown for stresses between 6000 and 8000 psi at each temperature.

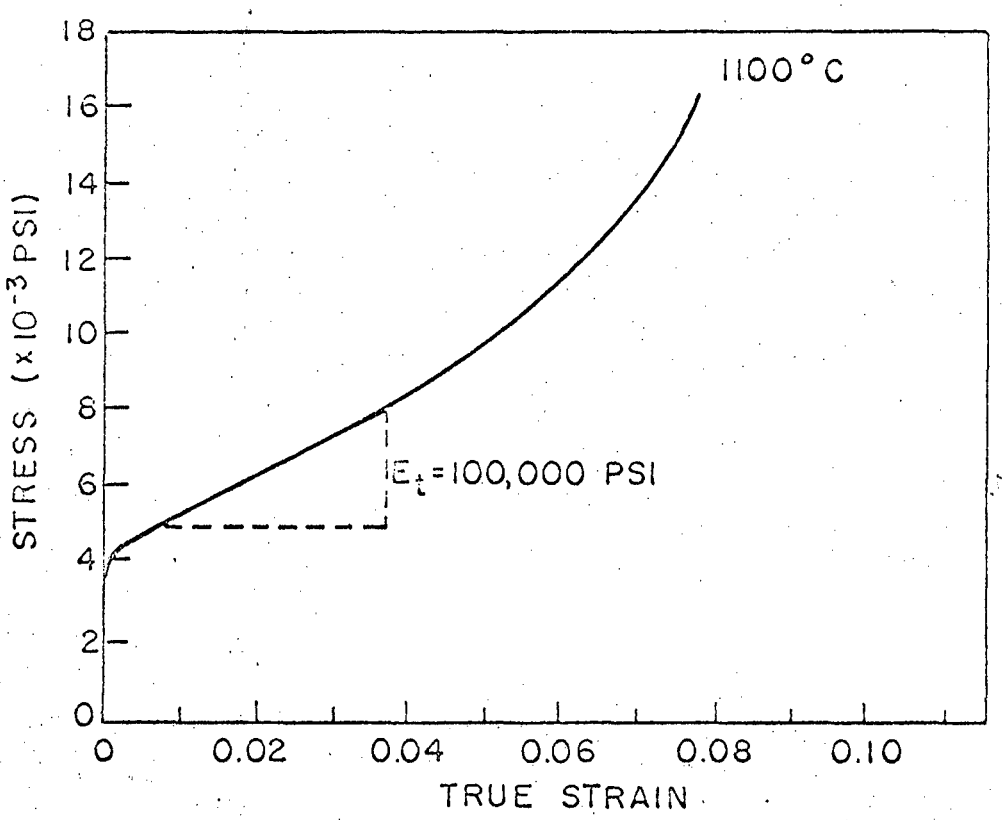
1100° C
E_t=100,000 PSI
STRESS (x10^{-3} PSI)
TRUE STRAIN
0
2
4
6
8
10
12
14
16
18
0
0.02
0.04
0.06
0.08
0.10

(b)

(Fig. 4)

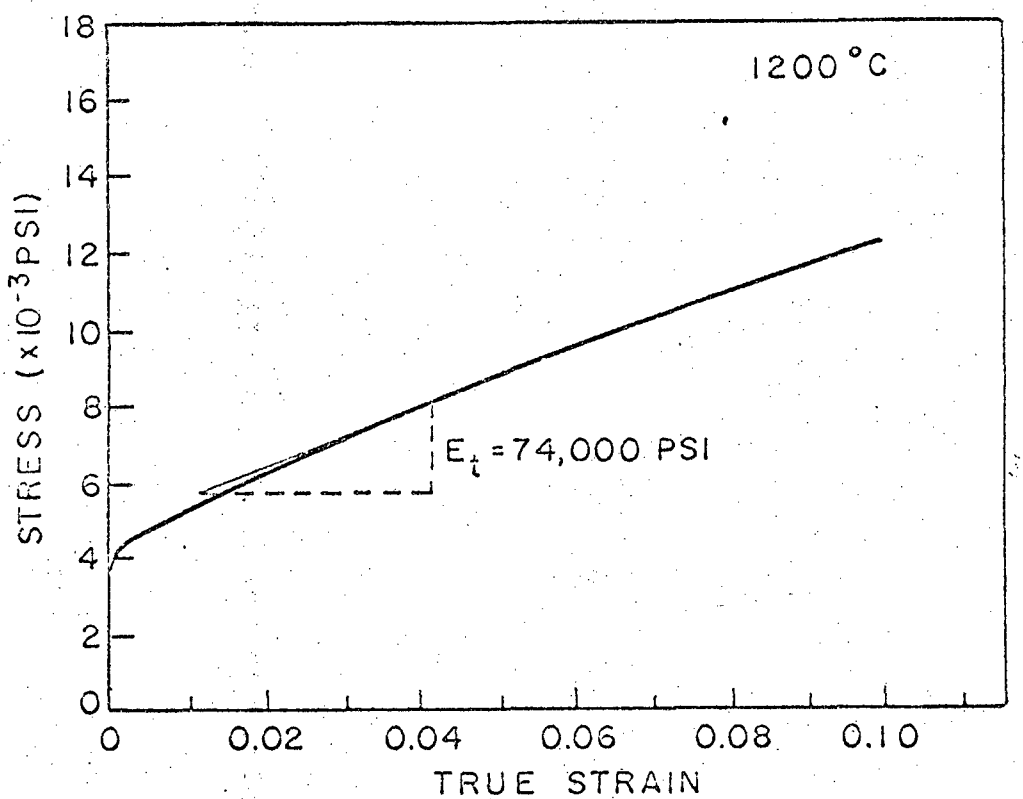
1200 °C
E_t = 74,000 PSI
STRESS ($\times 10^{-3}$ PSI)
TRUE STRAIN
0
2
4
6
8
10
12
14
16
18
0
0.02
0.04
0.06
0.08
0.10

(c)

(Fig. 4)

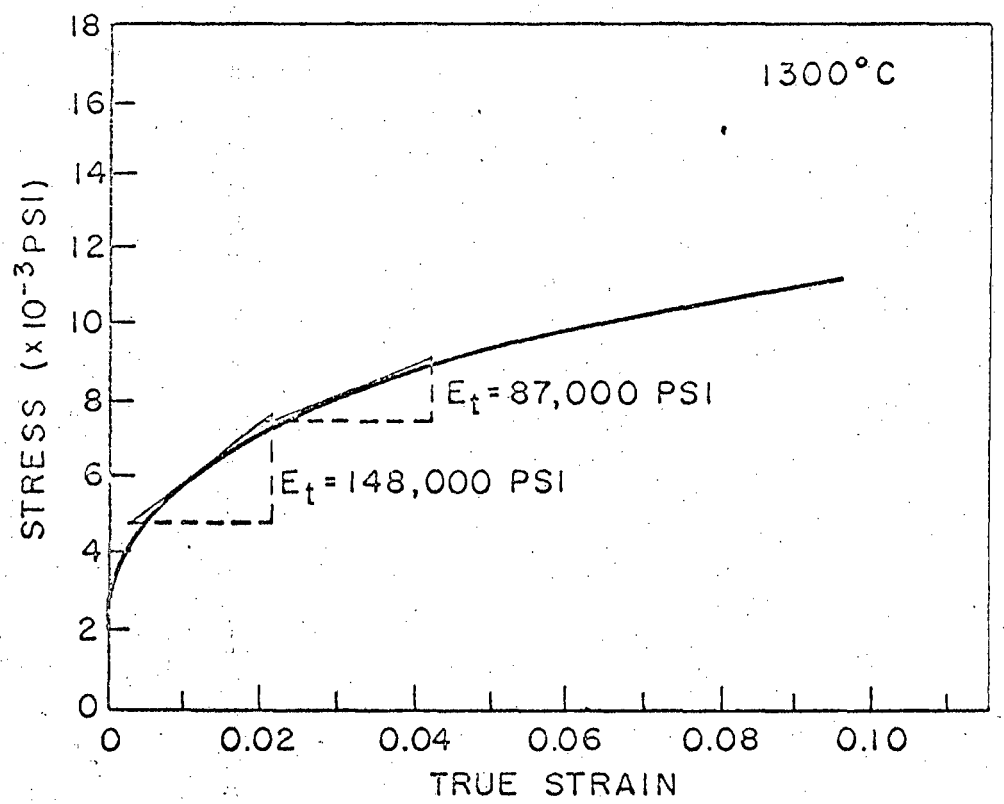
1300°C
STRESS (x10^{-3} PSI)
TRUE STRAIN
E_t = 87,000 PSI
E_t = 148,000 PSI
0
2
4
6
8
10
12
14
16
18
0
0.02
0.04
0.06
0.08
0.10

(d)

(Fig. 4)

Note the strong influence of the shape of the stress-strain curves on the buckling loads. At 1200°C and below the crystals yield abruptly causing a rapid reduction in the value of E_t just beyond the yield stress. As the axial load is increased beyond the level necessary for yielding, the probability of buckling thus increases rapidly. However, at the higher temperatures, e.g., 1300°C, the appearance of a gradual yield allows deformation to proceed as much as several percent before the possibility of buckling is introduced.

One important factor was omitted from the foregoing discussion--that of the end constraints characteristic of these experimental conditions. As was shown earlier for Eqs. (6)(a), (b), (c), the value of the critical load may vary between $1/4P_t$ and $4P_t$ where P_t is the value calculated for a column with pinned ends. It will be shown from the experimental results that it is unlikely that P_t for the conditions observed here is greater than about 2 times the value calculated for a column with pinned ends. It is noteworthy that the nature of the end constraints is critical, and that any increase in P_t will allow an increase in stress and strain before the possibility of buckling occurs.

Typical results from creep experiments performed between 1000° and 1300°C are shown in Fig. 5. The most striking feature of the data is the high degree of variability between tests performed under similar conditions. The straightforward explanation for this variability is that the occurrence of plastic buckling in the compressed MgO columns has introduced complications of stress distribution and consequently dislocation interactions. Careful examination of the deformed crystals confirmed this hypothesis.

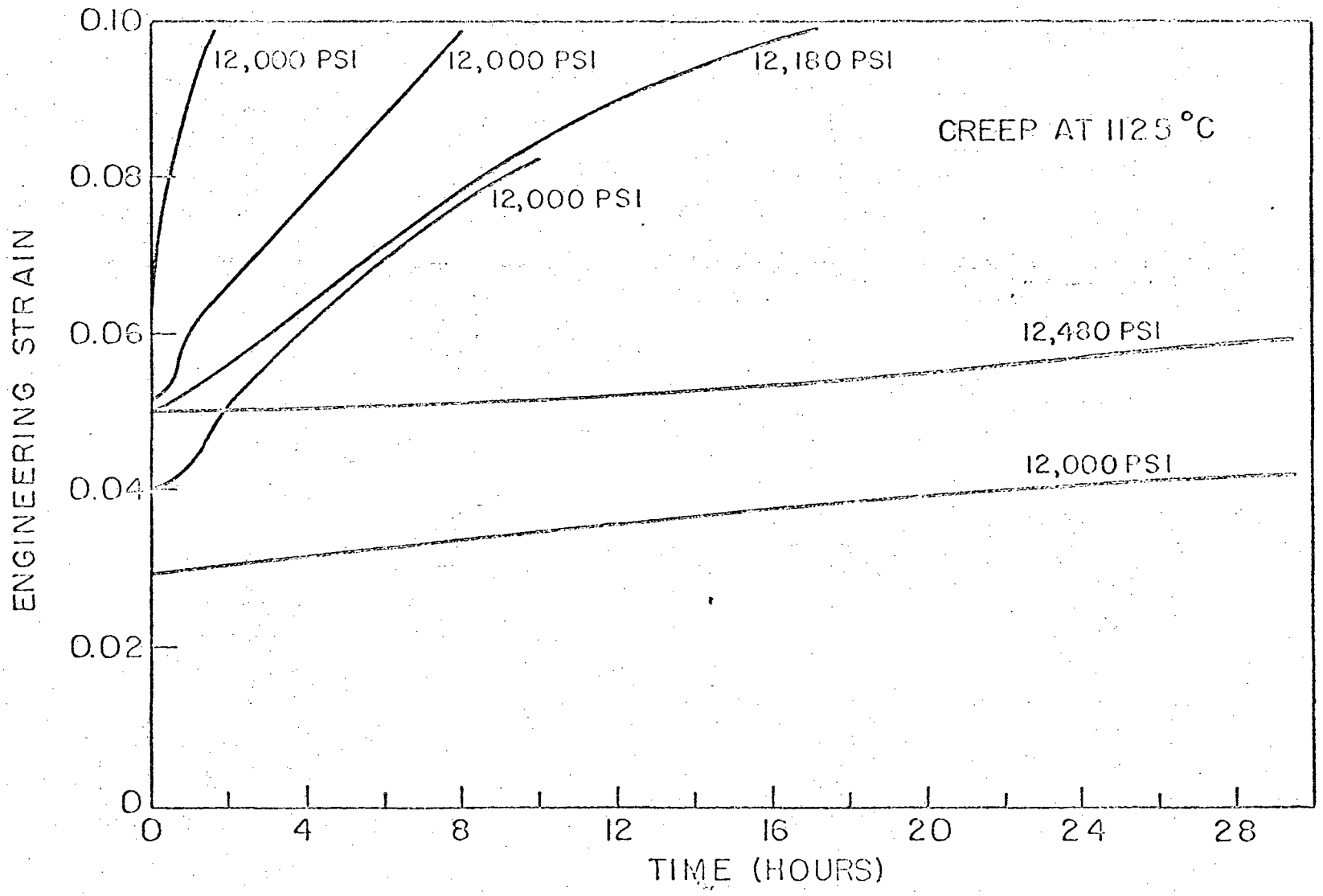

(a)

Fig. 5. Creep strain vs. time curves at 1125°, 1200° and 1300°C for single crystals compressed in an <001> direction. Values of stress are indicated on the respective curves.

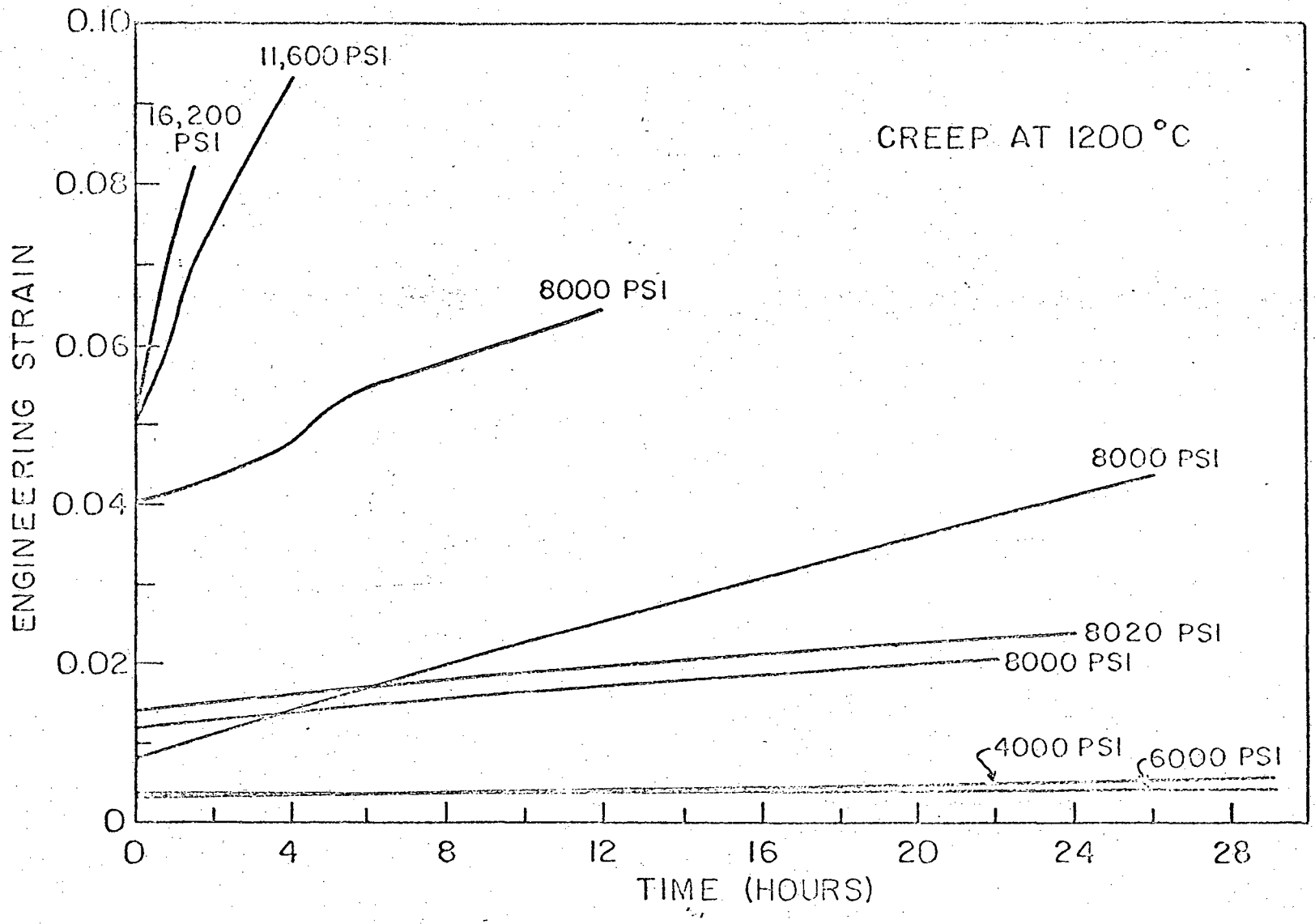
CREEP AT 1200 °C
ENGINEERING STRAIN
TIME (HOURS)
0.10
0.08
0.06
0.04
0.02
0
0
4
8
12
16
20
24
28
11,600 PSI
16,200 PSI
8000 PSI
8000 PSI
8020 PSI
8000 PSI
4000 PSI
6000 PSI

(b)

(Fig. 5)

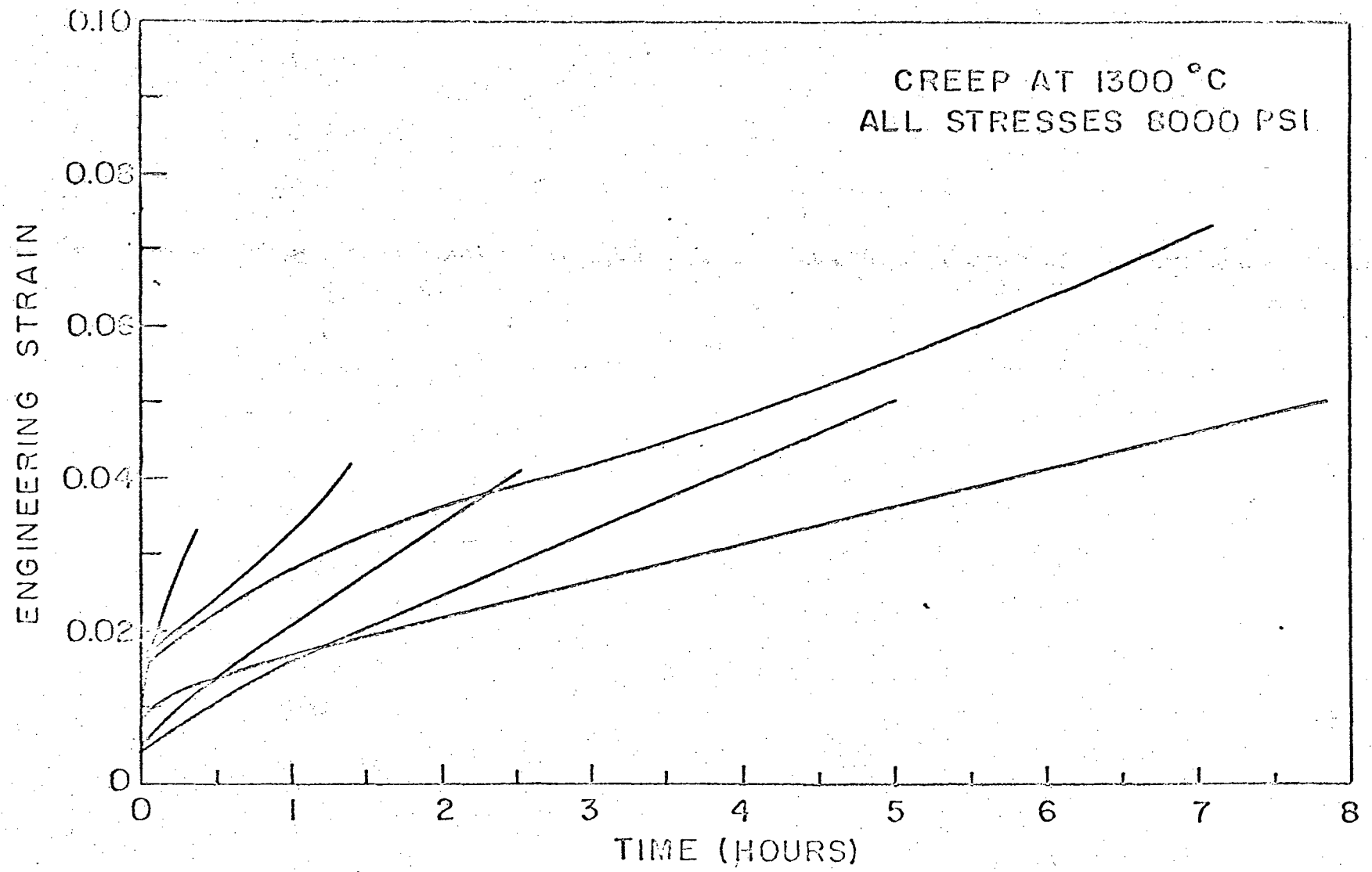
CREEP AT 1300 °C
ALL STRESSES 8000 PSI
ENGINEERING STRAIN
0.10
0.08
0.06
0.04
0.02
0
0
1
2
3
4
5
6
7
8
TIME (HOURS)

(c)

(Fig. 5)

Figure 6, for example, shows a crystal loaded to 13,150 psi at 1200°C that buckled quite severely. In general, the degree of buckling was not as great as that shown here; in some cases very close inspection of the crystal was required to confirm that buckling had in fact occurred. Figure 7 shows a crystal deformed at 1300°C and 8000 psi that apparently did not buckle; note the barrelled appearance indicative of fairly uniform deformation on a pair of conjugate $\{110\}\ \langle 1\bar{1}0\rangle$ slip systems.

B. Observations of Microstructure

Examination of the deformed crystals brought to light several interesting microstructural features. An etchant consisting of two parts H_3PO_4 and 1 part H_2SO_4 at room temperature was used to reveal etch pit patterns on the surface of deformed specimens. Since the tests were all performed at relatively high temperatures, the narrow well defined slip bands characteristic of low temperature deformation in MgO were not observed. Rather the more uniform, evenly distributed arrays of etch pits noted by Copley[21] were observed. Figure 8 shows the etched surface of a crystal deformed about 6% at 1300° and 8000 psi. This appearance is representative of etch pit patterns observed throughout the entirety of a deformed crystal.

In marked contrast to the uniform distribution of etch pits were the stress birefringence patterns obtained when viewing a deformed crystal between crossed polaroids. Although this technique presents more of a macroscopic view than etch pitting, considerable information as to the distribution and nature of slip can be obtained. One of the most striking features observed with this technique is the subdivision

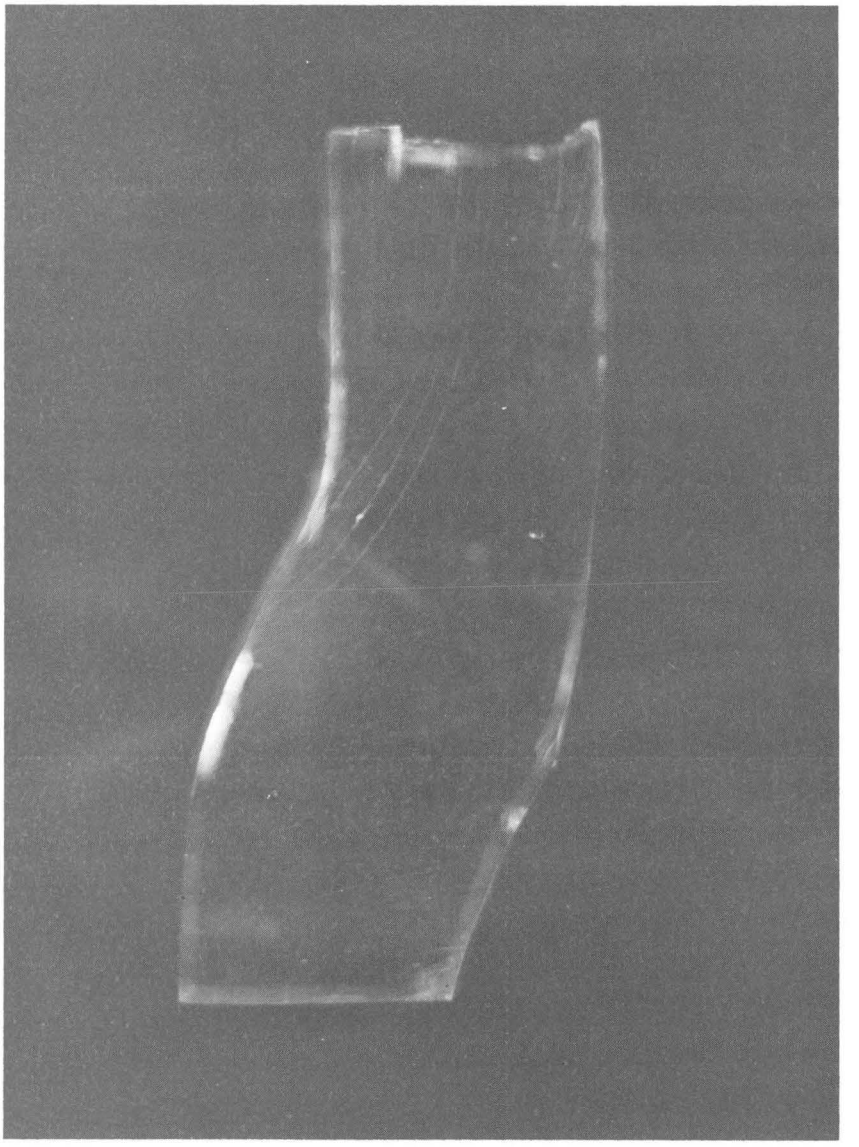

ZN-5900

Fig. 6. Crystal deformed about 16% at 1200°C and 13,000 psi showing extreme buckling.

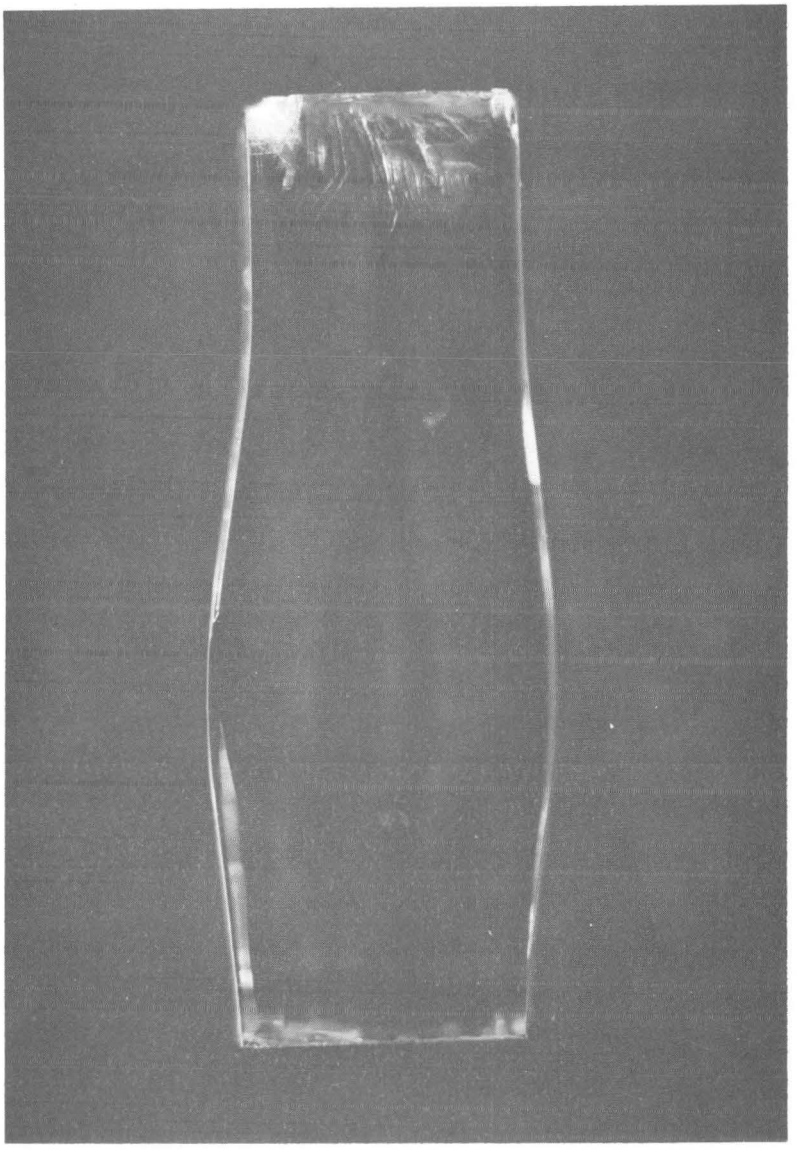

ZN-5901

Fig. 7. Crystal deformed about 16% at 1300°C and 8000 psi showing no buckling.

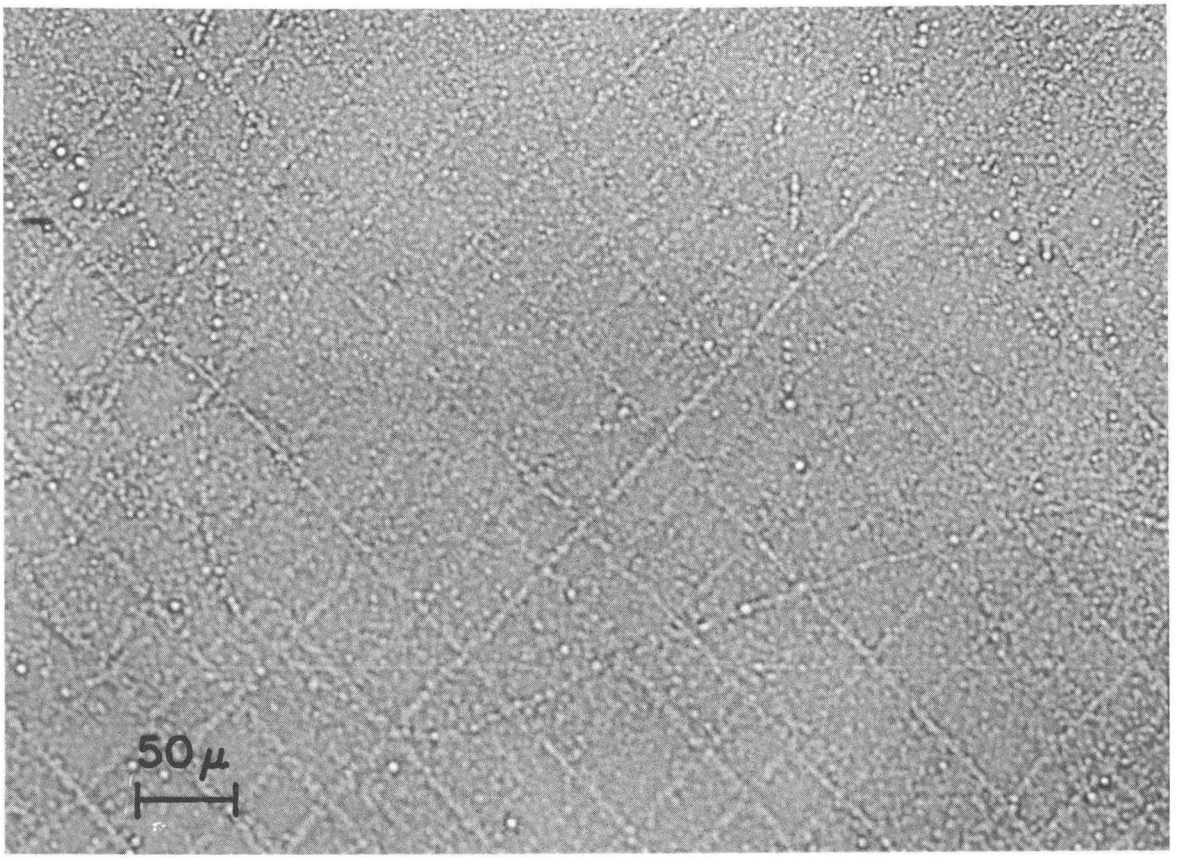

ZN-5902

Fig. 8. Polished and etched surface of a crystal deformed about 6% at 1300°C and 8000 psi.

of some crystals into blocks within which deformation proceeded by motion of separate {110} planes or conjugate pairs of {110} planes. Figure 9(a) shows an example of behavior of this type. The figure shows views of each of two adjoining {100} faces; it is seen that the crystal has subdivided into two blocks each containing deformation by motion on a single conjugate pair of {110} planes. This behavior is in contrast to that shown by the specimen in Fig. 9(b), also views of each of two adjoining {100} faces, which has deformed on a single pair of {110} planes over its entire length. Day and Stokes[5] observed the same phenomena in tensile loading at temperatures between 1300° and 1700°C. They attributed the behavior to difficulties in forcing intersections between {110} $\langle 1\bar{1}0 \rangle$ dislocations whose Burgers vectors lie at 120° to each other; interpenetration of dislocations at 90° was found to be complete. They found that below 1300°C the interpenetration of slip on orthogonal {110} planes was difficult. In this study, however, regions of complete interpenetration on orthogonal systems have been observed in crystals tested in compression at temperatures as low as 1100°C. It is reasonable to expect that compression testing, with more rigid ends, would tend to force intersections on orthogonal planes at lower temperatures than they would normally occur in tension.

C. Effect of End Constraints

To determine as closely as possible the nature of the end conditions existing in these experiments the following procedure was followed. It is possible to write the equation for the critical buckling load in the form

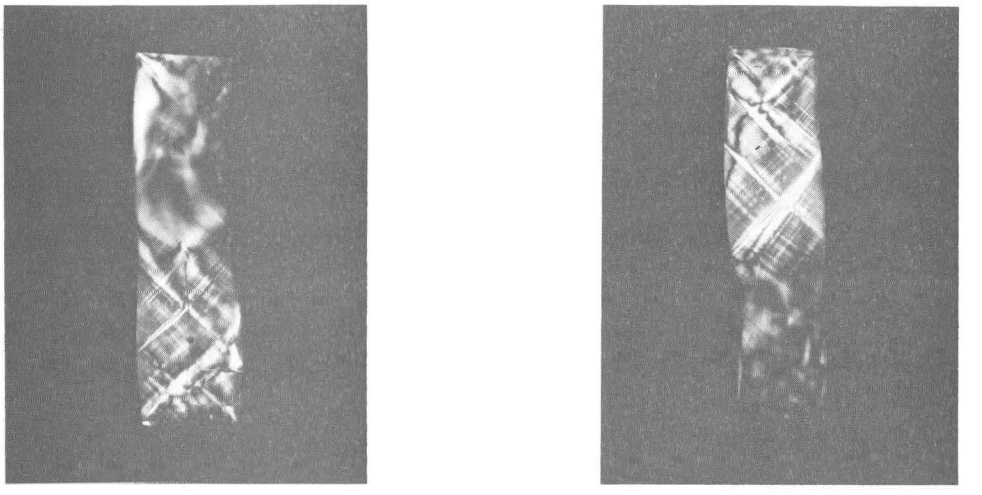

(a)

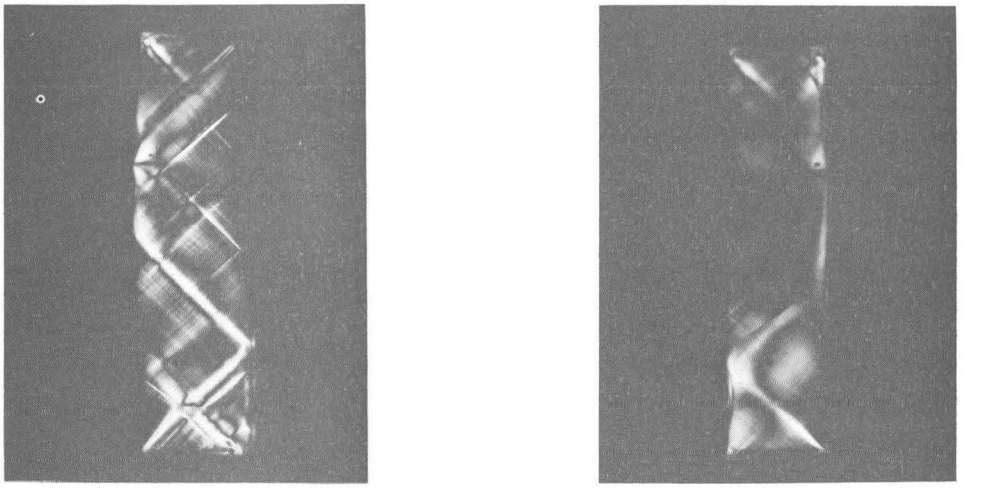

(b)

ZN-5899

Fig. 9. Specimens viewed between crossed polaroids with transmitted light showing (a) subdivision into separate blocks, and (b) no subdivision.

$$P_t = \beta \frac{\pi^2 E_t I}{L^2} \tag{9}$$

where β is a number characteristic of the end constraints for a given experiment. The value of β may vary between 0.25 and 4.0 as discussed in the introduction. For a crystal that has buckled we know that the applied load for the stress level involved exceeds P_t in Eq. (9). Thus by using this equation with the value of the applied load, the specimen geometry and the tangent modulus at that stress level, an approximate value of β can be calculated. By making this calculation for tests at the lowest stresses where buckling occurred, the minimum value of β is obtained. For example, a crystal that buckled at 1200°C and 6000 psi (304 lb. load) results in $\beta = 1.9$. Analogous calculations for other low stress experiments resulted in similar values for β. Numerically it thus appears that the end conditions are approaching the case shown in Fig. 3(b), a column fixed at one end and pinned at the other. Actually the situation is probably much more complicated but the illustration does appear qualitatively similar to some of the deformed specimens.

D. Stress Distribution in a Buckled Column

There does not appear to be a completely straightforward explanation for the behavior of a buckled bar under creep conditions. Hoffman and Sachs[16] contrast the stress and strain distribution in buckled bars for the two cases of buckling described previously. Figure 10(a) shows the two distributions for the case where axial load and bending moment are applied simultaneously. This distribution is contrasted with that in

Fig. 10(b) where the axial load is applied to its total value, at which time the bending moment appears. Note that for the second case during the application of the moment, strain reversal takes place over part of the cross section. It is highly likely that the first case, as represented by Fig. 10(a) applies under the conditions described here.

It is not completely clear how such a stress distribution might affect the observed strain rate. The motion of and interactions between dislocation line segments lying on the high stress side of the central fiber would probably be enhanced while the opposite situation might apply on the low stress side. As the degree of bending that can occur is limited to some extent by the end conditions, it is likely that once a buckled configuration is realized, deformation may proceed more slowly than in a column that remained straight.

In order to check this hypothesis several crystals with small length to width ratios were prepared for testing. As the length to width ratio is reduced the value of the critical buckling load increases well above that of the applied load, thus insuring that the column will remain unbuckled. However, it is difficult to obtain a single crystal specimen of such size that an appreciable volume of material is free to deform. Frictional forces encountered between the specimen ends and the loading rams effectively reduce the volume of material that can deform. Consider, for example, two crystals with dimensions as shown in Fig. 11. As the shaded area represents material not restricted by frictional forces, it is evident that the stubby crystal, Fig. 11(a), will appear "harder" in a compression than the slender column in Fig. 11(b). This difference was in fact confirmed by a creep test at 1200°C and

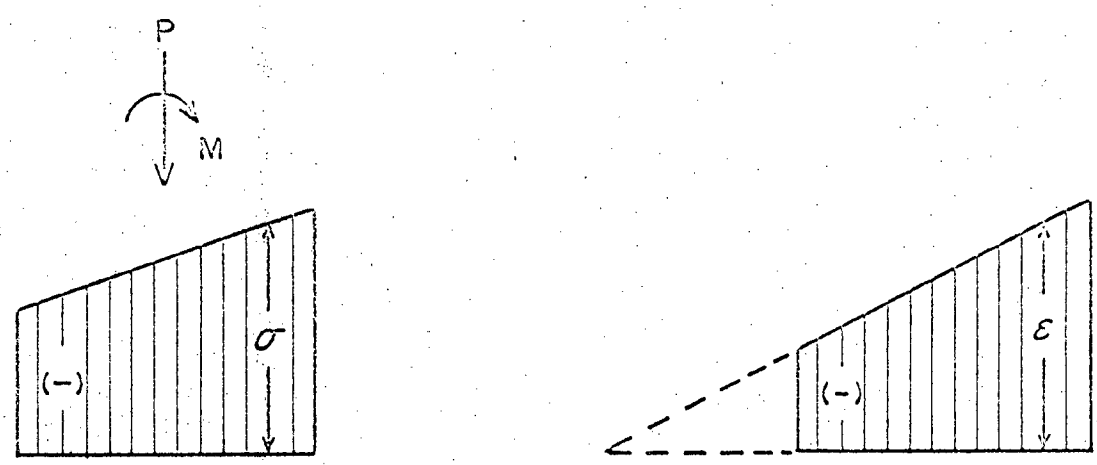

(a) CASE 1

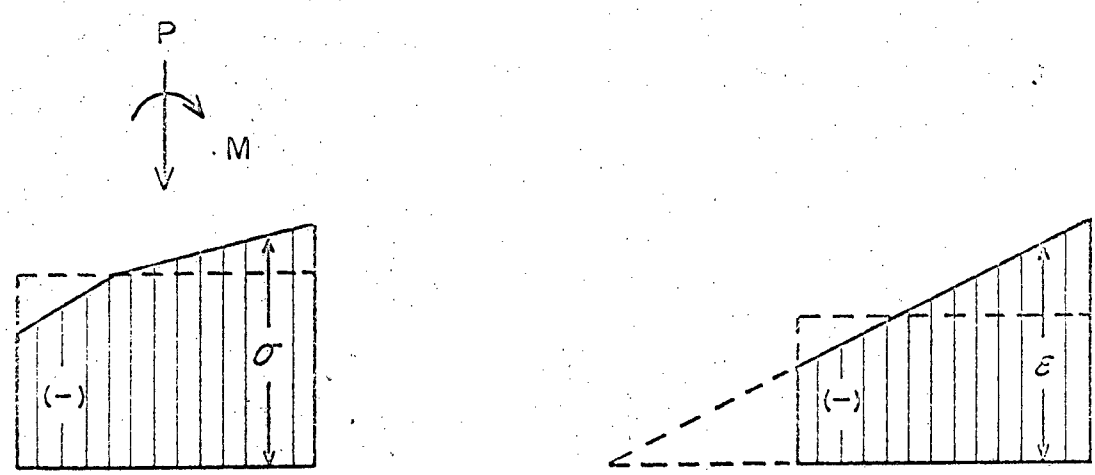

(b) CASE 2

Fig. 10. Stress and strain distributions in bars subjected to buckling, (a) case 1, and (b) case 2.

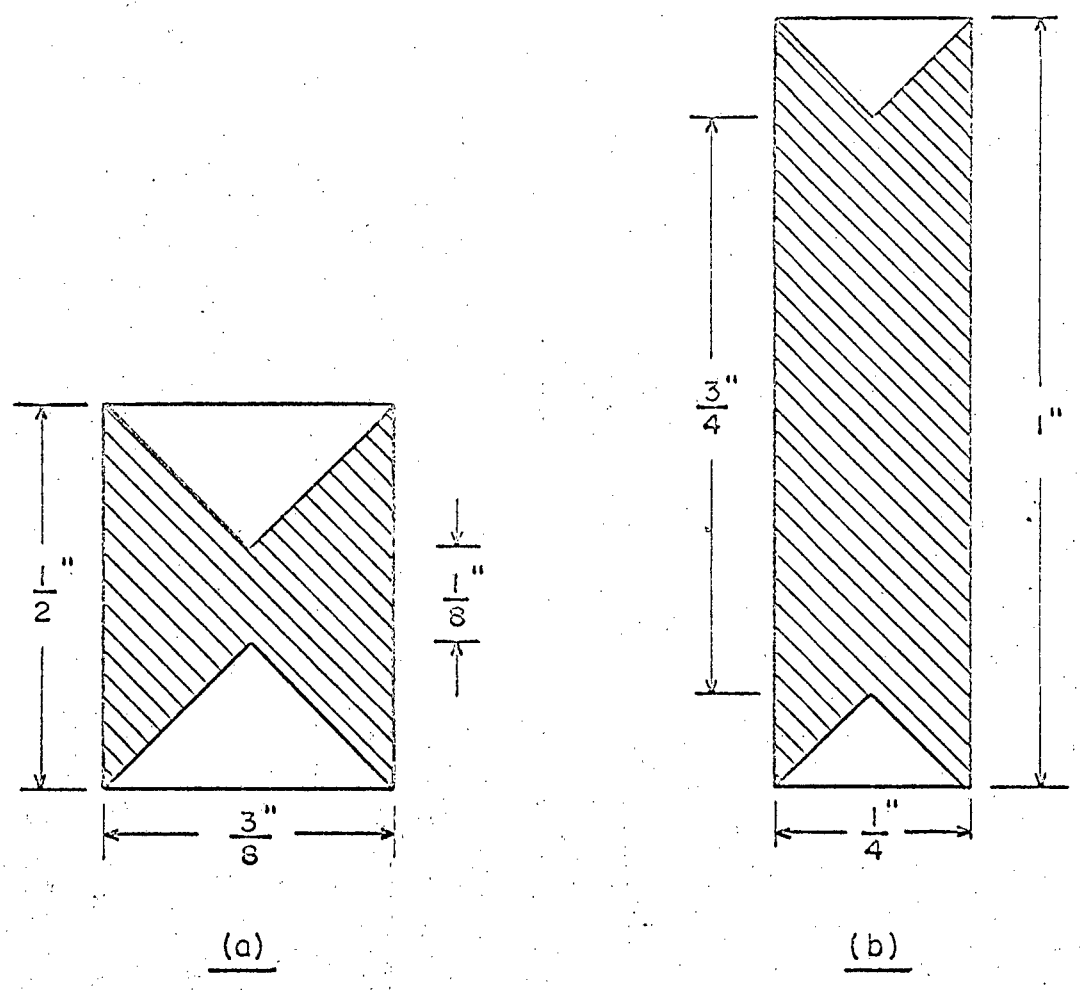

Fig. 11. Effect of specimen size on deformation in compression tests.

8000 psi utilizing a specimen having the dimensions shown in Fig. 11(a). The crystal did not deform readily and cracked quite severely during the test at a temperature and stress where normal specimens would have shown large strains and little tendency for cracking. Thus it was not possible to obtain a direct comparison between strain rates of straight and buckled columns.

E. Surface Condition

One feature of the mechanical behavior of MgO that has attracted much attention over the years is the effect of surface condition on ductility. It has been shown that at room temperature a chemical polishing treatment that removes fresh surface dislocations can cause the material to behave completely elastically up to fracture. As slip in MgO is considered to be initiated at sites of surface damage, the reduction in ductility is reasonable. However, some investigators, notably Copley[21] and Cass[22] have suggested that at elevated temperatures segments of the grown-in dislocation substructure may act as initiators of slip. To determine what effect, if any, this factor might have on creep, a series of experiments on crystals having extreme conditions of surface damage was performed. The two extreme conditions were a chemically polished (undamaged) surface and a polished and subsequently heavily damaged surface. Creep experiments at 1200° and 1300°C and 8000 psi gave the striking results shown in Fig. 12. At the lower temperature the degree of surface damage did not appear to have a significant influence on the strain rate. At 1300°C, however, the polished crystals consistently deformed at a higher rate than the heavily damaged specimens.

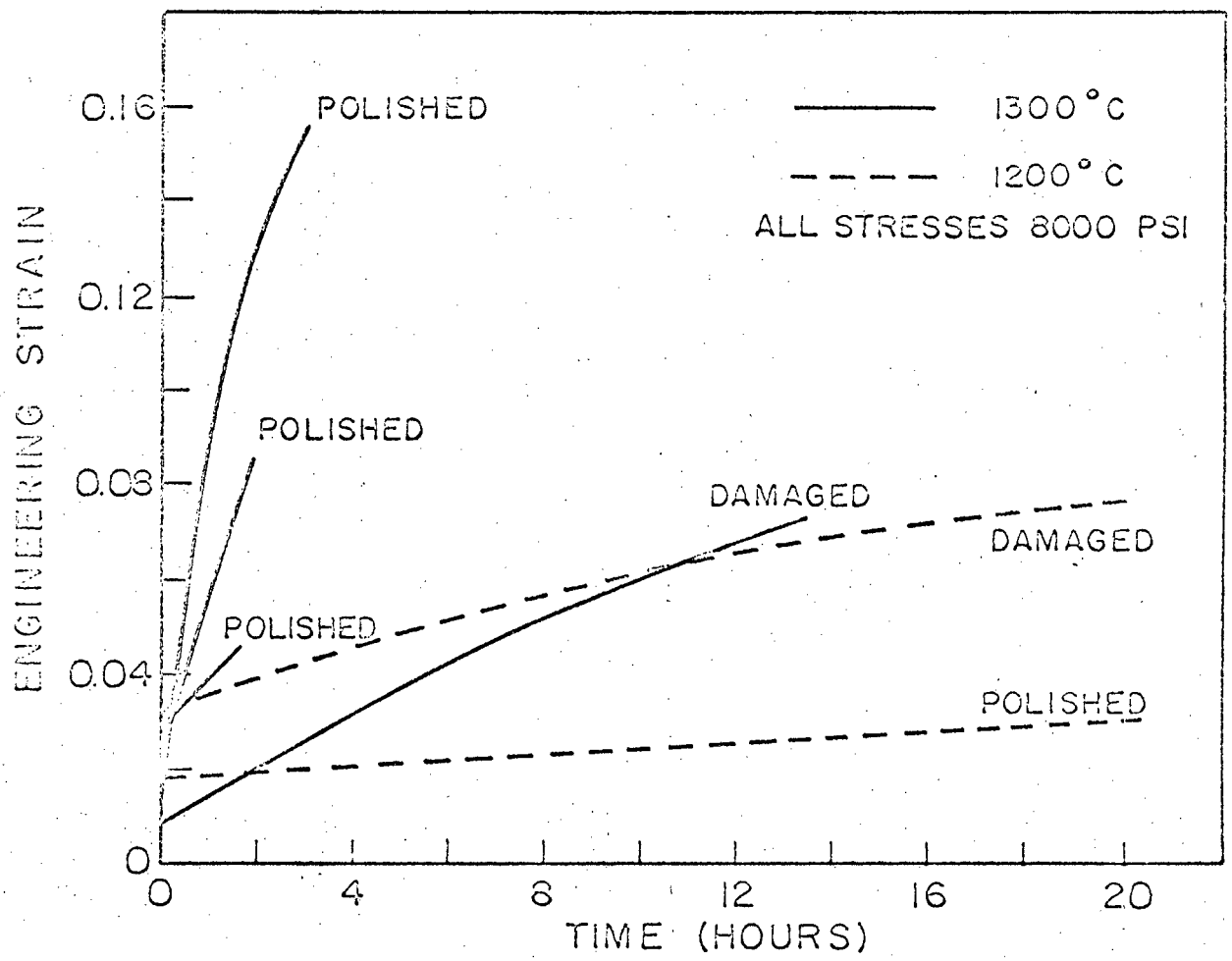

Fig. 12. Creep strain vs. time curves for a number of crystals with controlled surface conditions.

Apparently the heavy surface damage caused by dropping SiC grit on the crystals results in initiation of slip on so many intersecting {110} planes that the subsequent creep deformation is then limited. At 1200°C and below, grown-in dislocations cannot act as initiators of slip on a large scale; hence the low strain rate for the polished crystal. But at higher temperatures, the grown-in dislocations do initiate slip; this results in the higher strain rates observed for polished specimens at 1300°C. These results must be qualified, however, in that the buckling effect is actually superimposed on these tests. Nonetheless the experimental evidence presented suggests that the surface effects are real.

F. Mechanisms

1. Stress Exponent

It is possible to deduce from other trends in the data some information as to the nature of the mechanisms of creep in single crystal MgO. Many investigators have noted a change in deformation behavior at temperatures in the vicinity of 1200°C. Hulse, Copley and Pask,[9] for example, found a marked increase in total strain at fracture for <001> oriented crystals as the test temperature exceeded 1150°C. A calculation of one-half the melting point (in absolute degrees) yields a value of about 1240°C for MgO. As diffusional processes begin to contribute to appreciable deformation in the neighborhood of $0.5T_m$, several recently proposed mechanisms appear feasible. One such theory is that proposed by Weertman[12] for high temperature deformation controlled by climb of edge dislocations over barriers. Recently Chang[20] proposed a model for high temperature creep based on diffusion controlled dissolution of dislocation trails. A number of authors, Stokes[4] and

Cass[22] for example, have shown that the debris resulting from motion of dislocations in MgO at temperatures around 1000° to 1300°C is largely in the form of dislocation dipoles and prismatic loops.

Weertman originally proposed that the strain rate vs. stress relationship takes the form of a power law, i.e.

$$\text{creep rate} = \text{const} \left(\frac{\sigma}{kT}\right)^{\alpha} \exp\left(-\frac{Q}{kT}\right) \qquad (10)$$

where α is a constant ($\alpha \sim 3$ to 4), Q is the activation energy of self diffusion, σ is the applied stress, k is Boltzmann's constant and T is the absolute temperature. Chang's theory also predicts a power law relationship between strain rate and stress. He derives an equation of the same form as Eq. (10) but with the constant α being equal to 5 for dissolution of dipoles and 4 for dissolution of loops, respectively.

A series of tests were performed at 1200°C under various loads giving initial stresses from 4000 psi to 16,000 psi. Figure 13 is a log-log plot of strain rate versus stress; the line drawn through the data points has a slope of 4.7. This value is not at all unreasonable as Stokes[4] has shown 1200°C to be in the range of temperatures at which the slip band debris changes from dipoles to large prismatic loops. It is interesting to note that the logarithmic plot of strain rate versus stress appears to be relatively insensitive to the scatter introduced by buckling.

2. Activation Energy

Several different attempts were made to determine an activation energy for whatever process or processes are rate controlling but results were inconclusive. As buckling was occurring during most of these tests

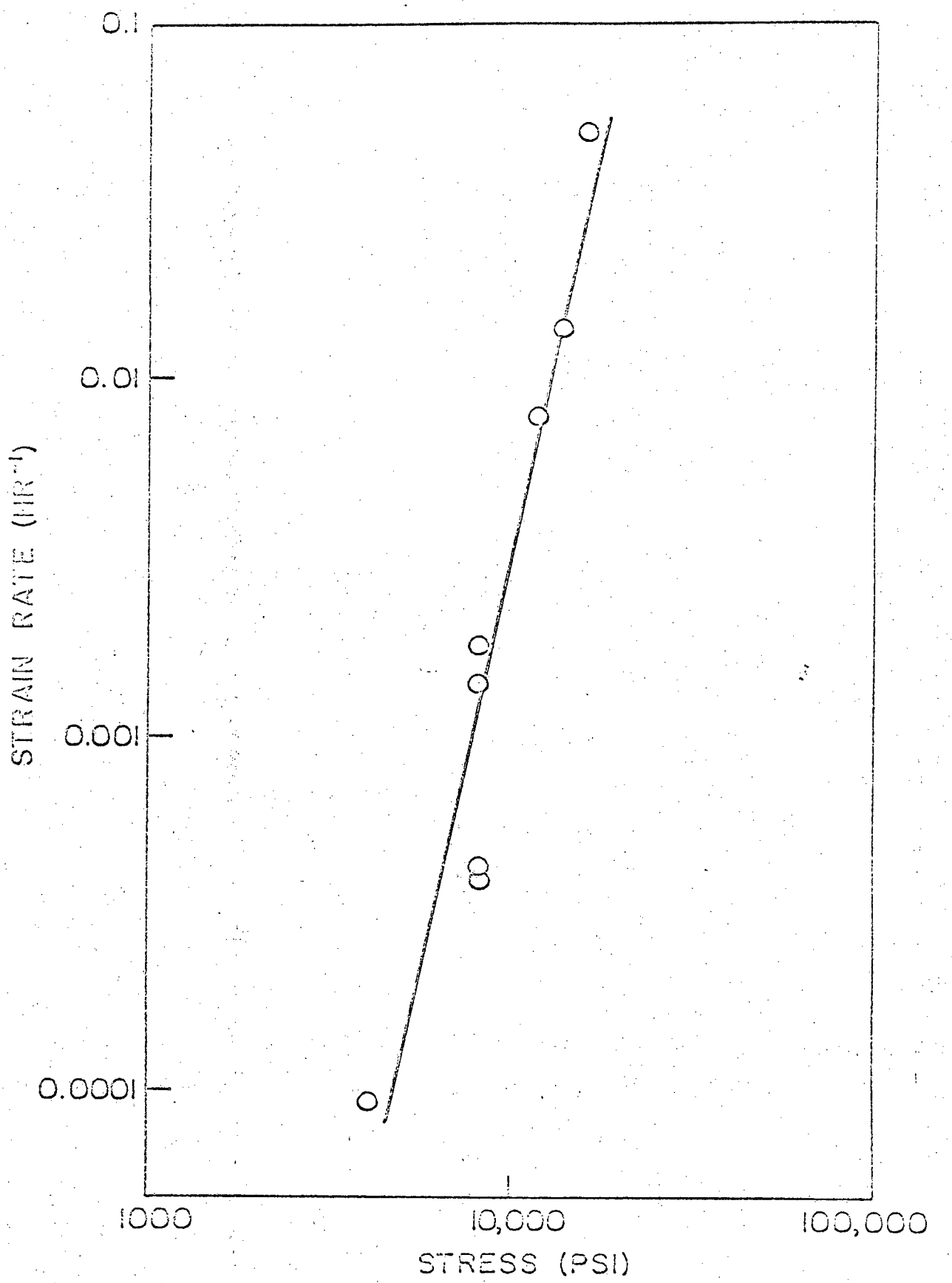

Fig. 13. Stress dependence of creep strain rate at 1200°C.

it is not unexpected that problems might occur. The primary method employed was that of inducing incremental changes in temperature and calculating the activation energy from the strain rates just prior and just after the change. Values of the activation energy obtained this way ranged from about 40 kcal/mole to about 300 kcal/mole. It would probably be a mistake to try and attribute any particular significance to these values as little is known about the exact nature of the stress or strain distribution and how it might have changed during the course of the test. Several normal Arrhenius plots of log strain rate versus reciprocal absolute temperature were made in an effort to obtain an activation energy. No significant values were obtained due to the large scatter of data points. Apparently the data plotted on a semilogarithmic Arrhenius basis (log strain rate versus reciprocal absolute temperature) is considerably more sensitive to variations introduced by buckling than was the stress exponent plot.

IV. CONCLUSIONS

Mathematical analyses and experimental observations have shown that slender single crystal MgO columns loaded in compression may be subject to plastic buckling. The nature of the end constraints may critically influence the stability of such a column in that the buckling load can change by a factor of 16 for various end conditions. For the temperature range studied here, (1000° to 1300°C), fewer than 5% of the columns were stable. This factor results in considerable uncertainty in interpreting the data or obtaining quantitative information concerning the creep mechanisms.

The deformed crystals exhibit extreme inhomogeniety with regard to distribution of slip. Etch pitting suggests that the damage is spread in a dense continuum of slip throughout the crystal. The actual nature of the damage, observed by viewing the crystal between crossed polaroids, was found to be markedly inhomogeneous. In extreme cases some crystals subdivided into separate blocks containing deformation on different conjugate pairs of $\{110\}\ \langle 1\bar{1}0\rangle$ slip systems.

Evidence was found that at temperatures exceeding about 1200°C segments of the grown-in dislocation substructure can act as initiators of slip. In particular, experiments at 1300°C appear to support this hypothesis despite the occurrence of plastic buckling.

From a series of tests at 1200°C it was found that the stress dependence of the creep rate can be expressed as a power law with a stress exponent of about 4.7. This value is in good agreement with Chang's theory of creep based on diffusion controlled dissolution of dislocation dipoles and loops. Experiments to determine the activation

energy for creep were largely inconclusive due to wide scatter in the data.

This study suggests that investigations of plastic deformation in compression are particularly sensitive to buckling because of a marked drop in the value of the tangent modulus after yielding. It is not clear at this point just how the shape of the stress-strain curve beyond the instability point is affected. The creep data suggests that a buckled column appears qualitatively "harder" than one which does not buckle. It is expected, however, that creep experiments, because of their constant stress level, may be particularly sensitive to stress pertubations caused by buckling.

ACKNOWLEDGMENTS

The author wishes to thank Professor Joseph A. Pask for his encouragement and guidance throughout the course of this study. Thanks are also due Norman E. Olson for his assistance in performing the mechanical tests.

This work was done under the auspices of the U. S. Atomic Energy Commission.

REFERENCES

1. E. R. Parker, Pages 78-80 in "High Temperature--A Tool for the Future.", Stanford Research Institute, Menlo Park, California, 1956.

2. A. E. Gorum, E. R. Parker, J. A. Pask, "Effect of Surface Condition on Room Temperature Ductility of Ionic Crystals," J. Am. Ceram. Soc. 41 [5] 161-64 (1958).

3. R. J. Stokes, "Thermal-Mechanical History and the Strength of Magnesium Oxide Single Crystals: I, Mechanical Tests," J. Am. Ceram. Soc., 48 [2] 60-67 (1965).

4. R. J. Stokes, "Thermal-Mechanical History and the Strength of Magnesium Oxide Single Crystals: II, Etch Pit and Electron Transmission Studies," J. Am. Ceram. Soc., 49 [1] 39-46 (1966).

5. R. B. Day, R. J. Stokes, "Mechanical Behavior of Magnesium Oxide at High Temperatures," J. Am. Ceram. Soc., 47 [10] 493-503 (1964).

6. R. B. Day, R. J. Stokes, "Effect of Crystal Orientation on the Mechanical Strength of Magnesium Oxide at High Temperatures," J. Am. Ceram. Soc. 49 [2] 72-80 (1966).

7. A. E. Gorum, W. J. Luhman, and J. A. Pask, "Effect of Impurities and Heat-Treatment on Ductility of MgO," J. Am. Ceram. Soc. 43 [5] 241-245 (1960).

8. C. O. Hulse, J. A. Pask, "Mechanical Properties of Magnesium Oxide Single Crystals in Compression", J. Am. Ceram. Soc. 43 [7] 373-78 (1960).

9. C. O. Hulse, S. M. Copley, and J. A. Pask, "Effect of Crystal Orientation on Plastic Deformation of Magnesium Oxide," J. Am. Ceram. Soc., 46 [7] 317-323 (1963).

10. S. M. Copley and J. A. Pask, "Plastic Deformation of MgO Single Crystals up to 1600°C," J. Am. Ceram. Soc. 48 [3] 139-146 (1965).

11. R. L. Cummerow, "High-Temperature Steady-State Creep Rate in Single Crystal MgO", J. Applied Physics 34 [6] 1724-1729 (1963).

12. J. Weertman, "Theory of Steady-State Creep Based on Dislocation Climb," J. Appl. Phys. 26 [10] 1213-1217 (1955).

13. A. S. Neiman and W. S. Rothwell, "Effect of an Electric Field on Creep of MgO Single Crystals," Appl. Phys. Letters, 3 [9] 160-61 (1963).

14. W. S. Rothwell, A. S. Neiman, "Creep in Vacuum of MgO Single Crystals and the Electric Field Effect," J. Appl. Phys. 36 [7] 2309-2316 (1965).

15. W. S. Rothwell, "Analysis of Time-Dependent Creep Phenomena in Single Crystal MgO", J. Appl. Phys. 37 [7] 2833-2837 (1966).

16. O. Hoffman, and G. Sachs, "Introduction to Theory of Plasticity for Engineers,"pp. 142-147, McGraw-Hill Book Co., Inc., New York 1953.

17. F. R. Shanley, "Inelastic Column Theory," J. Aeronaut. Sci, 14 [5] 261-268 (1947).

18. E. P. Popov, Mechanics of Materials, pp. 346-348, Prentice-Hall, Inc., Englewood Cliffs, N.J., 1952.

19. C. O. Hulse and S. M. Copley, "High Temperature Compressive Deformation Equipment", UCRL-16434, Lawrence Radiation Laboratory, Berkeley, California, 1965.

20. R. Chang, "Dislocation Theories of the High Temperature Creep of Crystalline Solids," The Physics and Chemistry of Ceramics, pp. 275-285, Gordon and Breach, New York, 1963.

21. S. Copley, "Plastic Deformation of Magnesium Oxide Single Crystals at Elevated Temperatures," (Thesis) UCRL-11323, Lawrence Radiation Laboratory, Berkeley, California, (1964).

22. T. Cass, "Dislocation Dipoles in Deformed Magnesium Oxide", UCRL-11996, Lawrence Radiation Laboratory, Berkeley, California, (1965).

This report was prepared as an account of Government sponsored work. Neither the United States, nor the Commission, nor any person acting on behalf of the Commission:

A. Makes any warranty or representation, expressed or implied, with respect to the accuracy, completeness, or usefulness of the information contained in this report, or that the use of any information, apparatus, method, or process disclosed in this report may not infringe privately owned rights; or

B. Assumes any liabilities with respect to the use of, or for damages resulting from the use of any information, apparatus, method, or process disclosed in this report.

As used in the above, "person acting on behalf of the Commission" includes any employee or contractor of the Commission, or employee of such contractor, to the extent that such employee or contractor of the Commission, or employee of such contractor prepares, disseminates, or provides access to, any information pursuant to his employment or contract with the Commission, or his employment with such contractor.